DOI: 10.61782/fa.2025.0890

FORUM ACUSTICUM
EURONOISE 2025

THE SPATIO-TEMPORAL AND FREQUENCY MODELING OF DEEP-SEA SURFACE REVERBERATION CAUSED BY DIFFERENT WAVEFORMS

Xiaomei Wang[2] **Xingyuan Pei**[1]* **Xiaochuan Ma**[1]
Chao Feng[1] **Yu Liu**[1]
[1] Institute of Acoustics of the Chinese Academy of Sciences, Beijing, China
[2] National Satellite Ocean Application Service, Beijing, China

ABSTRACT

The near-seabed sonar in deep sea can provide positioning signals for underwater unmanned vehicles in the region, and can also provide traffic management services for underwater vehicle clusters in the area. However, the sea surface reverberation caused by the navigation communication signal emitted by the near-seabed sonar may drown the response signal of the underwater vehicle and interfere with the seabed sonar's estimation of the position of the underwater vehicle. We analyze the spatio-temporal and frequency distribution characteristics of sea surface reverberation caused by different types of navigation signals, which provides support for the design of collaborative communication signals and cluster interaction management protocols for unmanned underwater systems.

Keywords: *deep sea, reverberation modeling, point scattering model*

1. INTRODUCTION

Under harsh deep-sea meteorological conditions, maritime transport vessels and crew safety face significant threats. Future unmanned surface transport vessels, semi-submerged transport vessels, and even sub-surface navigation vehicles could substantially mitigate maritime risks and economic costs. Oceanographic satellites enable continuous monitoring of sea surface wave height, wave number, and meteorological forecasting, thereby enhancing safety management for surface fleets. For sub-surface unmanned vessels, sonar-assisted navigation and management systems are essential. Deep-sea sonar arrays deployed near the seabed can service extensive areas.

The direct path sound rays corresponding to the sonar deployed at a depth of 5000 meters and detecting upwards are shown in Fig. 1. According to Fig. 1, the sonar deployed at a depth of 5000 meters can cover a horizontal distance of up to 30 km. Deep-sea navigation management sonar requires autonomous intelligence capabilities. Research on underwater environmental characteristics and vessel responses to sonar signals, coupled with the development of accurate datasets or data models, will facilitate the training of intelligent sonar algorithm systems.

Currently, most research focuses on underwater targets passive detection using sonar deployed in deep-sea environments [1, 2]. However, when the target exhibits low source levels, the passive detection approach faces limitations in detection range. To address these shortcomings, active detection has begun to attract attention [3]. When monostatic sonar systems deployed near seabed in deep sea actively detect underwater targets(as illustrated in Fig. 1), reverberation is the main interference that limits the capabilities of intelligent sonar services. Given the prohibitive costs associated with acquiring real-world deep-sea reverberation data for training intelligent sonar algorithms, it becomes imperative to develop a reverberation modeling framework to synthesize such datasets.

Long-term satellite data accumulation enables the es-

*Corresponding author: peixingyuan@mail.ioa.ac.cn.

tablishment of refined models for predicting deep-sea acoustic propagation paths. By integrating these acoustic propagation models with natural environmental parameters, it becomes feasible to accurately forecast underwater reverberation generated by active sonar signals. This predictive capability provides critical data support for the design optimization of near-seabed sonar systems. The proposed modeling approach facilitates the generation of high-fidelity reverberation datasets, thereby advancing the development of intelligent algorithms for target discrimination in deep-sea environments.

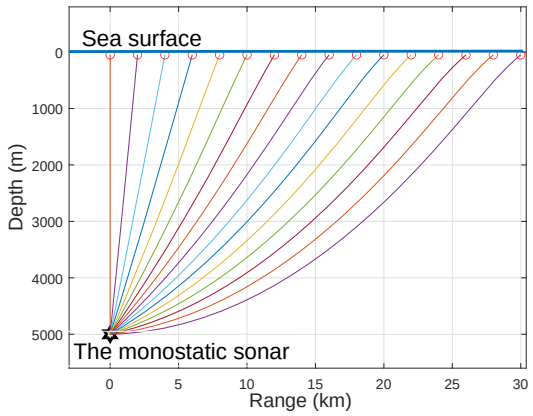

Figure 1. The diagram of looking upward from the bottom.

2. DEEP SEA REVERBERATION ANALYSIS

The reverberation model used to provide reverberation simulation data for intelligent sonar in deep-sea areas relies on three types of data support. The first is marine meteorological data. The second is geographic data in the sonar operational area. The third is sonar parameters. The reverberation model describes the mapping relationship between the aforementioned three types of data and the output reverberation data, as illustrated in Fig. 2. China's currently operational oceanographic satellites in orbit include the HY-2B/C/D series and the China-France Oceanography Satellite (CFOSAT), with data services provided by the National Oceanic Satellite Application Center. Marine geospatial information data are systematically curated and disseminated by the National Marine Data Center of China. Real meteorological and geographic information data for regions of interest can be obtained from these sources, allowing for the construction of reliable reverberation data. The subsequent sections of this chapter will analyze the correspondence between the aforementioned three types of data and reverberation data based on ray theory.

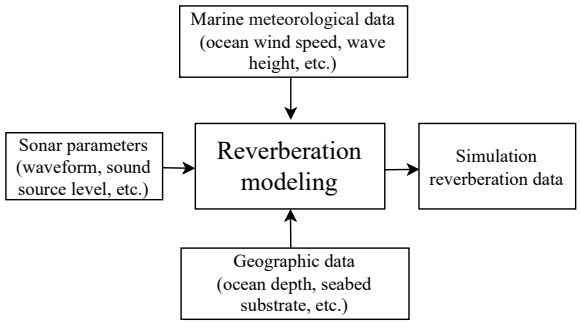

Figure 2. Deep sea reverberation construction model.

2.1 Analysis of the Reverberation Level of Deep-Sea Interface Reverberation

In underwater acoustic detection, the sonar equation under reverberation-limited conditions is formulated as

$$\mathrm{SL} - 2\mathrm{TL} + \mathrm{TS} - \mathrm{RL} > \mathrm{DT}, \tag{1}$$

where SL is Source Level, TL is Transmission Loss, TS is Target Strength, RL is Reverberation Level, DT is Detection Threshold. Through the analysis of the sonar equation, RL is an important parameter for detecting targets. In deep-sea environments, the received reverberation is primarily interface backscattering reverberation, and the calculation formula for the RL at a certain moment is

$$\mathrm{RL} = \mathrm{SL} - 2\mathrm{TL} + 10\lg(S) + S_{b/s}, \tag{2}$$

where S denotes the effective scattering area contributing to reverberation; $S_{b/s}$ represents the backscattering reverberation intensity per unit area from sea surface or seabed scatterers. The diagram of the interface backscattering reverberation is shown in Fig. 3.

In deep-sea active target detection scenarios, SL is known and sound waves are spherical expansion, TL is expressed as:

$$\mathrm{TL} = 20\lg(r) + \alpha r, \tag{3}$$

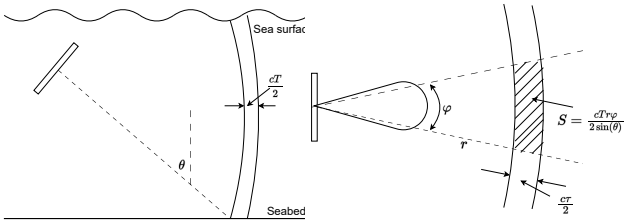

(a) (b)

Figure 3. Interface backscatter reverberation. (a) Side view; (b) Top vew.

where r represents the one-way acoustic propagation distance between the source and target, and α denotes the acoustic absorption coefficient. As shown in Fig. 3, the effective scattering area contributing to reverberation is denoted as:

$$S = \frac{cT}{2\sin(\theta)} r\varphi, \tag{4}$$

where φ denotes the beam horizontal opening angle, T represents the transmitted waveform pulse width, and θ corresponds to the pitch angle of reverberation (measured from the vertical axis). $S_{b/s}$ is governed by marine environmental parameters, sea surface backscattering strength (S_s) and seabed backscattering strength (S_b) employ distinct theoretical formulations.

2.2 The backscattering strength of interface reverberation

Due to the large scale of the deep sea, the range of grazing angles for the reverberation received by the hydrophone at the deep sea interface is very broad. Therefore, it is necessary to select a scattering function suitable for a wide range of grazing angles.

Regarding sea surface reverberation, Chapman et al. [4] derived an empirical model formula for sea surface reverberation backscattering strength, shown in Eqn. (5).

$$\begin{aligned} S_{CH} &= 3.3\beta \lg(\tfrac{\theta}{30}) - 42.4 \lg \beta + 2.6 \\ \beta &= 107(v f^{1/3})^{-0.58} \end{aligned}, \tag{5}$$

where S_{CH} is sea surface backscattering strength, θ is grazing angle(°), v is wind speed (m/s), f is the sound wave's frequency(Hz). Eqn. (5) is referred to as the Chapman model. The Chapman model is applicable in scenarios where the frequency meets 0.4 kHz $< f <$ 6.4 kHz and the grazing angle meets $\theta < 40°$. Ainslie, Ellis and Crowe modified the Chapman model to work with all grazing angles. The modified formula is

$$\begin{aligned} S_s &= 10 \lg \left[\sigma_{CH}(\theta) + \frac{e^{-\cot^2(\theta)/(2\xi^2)}}{8\pi\xi^2 \sin^4(\theta)} \right] \\ \xi^2 &= 0.003 + 0.00512v \end{aligned}, \tag{6}$$

where S_s is modified sea surface backscattering strength, $\sigma_{CH}(\theta) = 10^{S_{CH}/10}$. According to Eqn. (6), the sea surface reverberation backscattering strength under different frequencies and wind speeds is shown in Fig. 4. Accord-

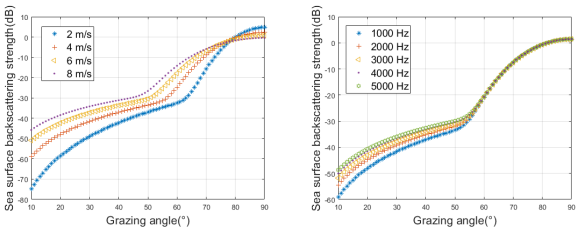

(a) (b)

Figure 4. Sea surface backscattering strength (unit: dB) as a function of grazing angle (unit: degrees) for various wind speeds and acoustic frequency is 2000 Hz in (a), for various acoustic frequencies and wind speed is 5 m/s in (b).

ing to Fig. 4, under the same conditions, the greater the wind speed or the sound wave's frequency, the larger the backscattering strength of the sea surface reverberation; the larger the grazing angle, the greater the backscattering strength of the sea surface reverberation.

Regarding seabed reverberation, this paper employs the GABIM [5] to calculate the seabed reverberation backscattering strength. The GABIM model interpolates various scattering theories, enabling the model's applicability under full grazing angles and diverse seabed substrate conditions. The GABIM model is applicable in scenarios where the frequency meets 100 Hz $< f <$ 10 kHz. In this paper, a simplified form of the seabed model is chosen, assuming that the seafloor is a single-layer liquid infinite half-space with a rough interface. The reverberation of seafloor scattering is mainly composed of seafloor rough interface scattering reverberation and volumetric scattering reverberation of sedimentary layers [6], and the simplified model of GABIM [5] calculates the

backscattering strength of seafloor reverberation as

$$S_b = 10\lg\left[\sigma_r(a_\rho, v_p, \alpha_\lambda, \omega_2, \gamma_2) + \sigma_v(a_\rho, v_p, \alpha_\lambda, \sigma)\right], \tag{7}$$

where σ_r and σ_v represent the backscattering strengths induced by the roughness of the water-sediment interface and the volume inhomogeneity of the sediment-substrate system, respectively. The formula for calculating σ_r is described in [5] and the formula for calculating σ_v is described in [7]. Tab. 1 lists the parameters required for the GABIM model of several common seabed substrates.

Table 1. Input parameters of the GABIM model under several typical substrate types.

Name	M_z	a_p	v_p	α_λ	ω_2	γ_2	σ
Clay	9.0	1.40	0.99	0.10	0.000016	3.25	0.001
Fine sand	2.5	1.94	1.15	0.89	0.000086	3.25	0.002
Pebble	-4	2.50	1.57	1.53	0.000458	3.25	0.002

The reverberation backscattering strength with different seabed substrates and frequencies is illustrated in Fig. 5. As shown in Fig. 5, the reverberation backscattering strength varies with different substrates, and it increases with the increasing reverberation grazing angle.

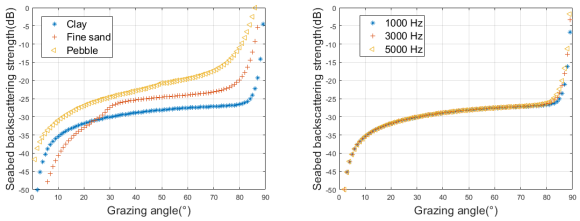

(a) (b)

Figure 5. Seabed backscattering strength (unit: dB) as a function of grazing angle (unit: degrees) for different substrates and acoustic frequency is 2000 Hz in (a), for different frequencies and the substrate is clay.

2.3 Analysis of Deep Sea Reverberation Spatiotemporal Structure

When a monostatic sonar is deployed near the seabed in deep sea to detect underwater targets, assuming horizontally uniform sea surface and seabed , the reverberation signals received by the hydrophone can be partitioned into three temporal intervals: early, intermediate, and late stages. Schematic diagrams of dominant reverberation paths corresponding to these intervals are illustrated in Fig. 6.

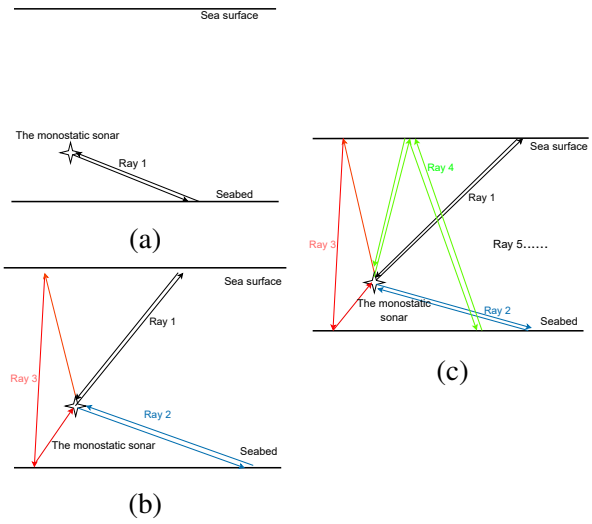

Figure 6. The reverberation paths received by the hydrophone at different time periods. (a) Early reverberation; (b) Middle reverberation; (c) Late reverberation.

In Fig. 6, the dominant reverberation paths contributing to the received echoes are illustrated for the three temporal intervals. Let t_1 and t_2 be the demarcation times of Fig. 6 (a), (b) and (c). Given that the distance of sonar from the seabed is much smaller than the the sea surface. t_1 Let t_1 denote the arrival time of reverberation originating directly from the sea surface at the receiving hydrophone, and t_2 represent the arrival time of sea-surface-reflected reverberation after a single interaction. During the $0 - t_1$ interval, the received reverberation predominantly originates from seabed backscattering, shown in Fig. 6(a). Since interesting targets are located near the sea surface, this interval generally contains no detectable targets except for potential objects directly above the hydrophone during its final phase. Consequently, reverbera-

tion within this temporal window exhibits negligible impact on target detection performance. During the $t_1 - t_2$ interval, the reverberation paths are shown in Fig. 6(b). The reverberation in this temporal window comprises not only direct-path backscattering from the seabed and sea surface but also single-bounce reflections involving either the sea surface or seabed interfaces. During the $t_2 - \infty$ interval, the reverberation paths are illustrated in Fig. 6(c). The reverberation in this temporal window comprises energetically dominant direct-path and single-bounce reflections, as well as weaker contributions from multiple-bounce multipath reverberation involving repeated interactions with the sea surface or seabed interfaces.

The arrival time delay and arrival angle of deep-sea reverberation can be calculated using the measured sound speed profile in conjunction with ray model, and the specific calculation method can be found in reference [8]. In order to analyze the multi-path structure of reverberation, the simulation environment is as follows: The ocean depth is 3000 m. The monostatic sonar depth is 2900 m. Assuming that the deep sea is isovelocity and the speed of sound is 1500 m/s. The sonar emits omnidirectionally, with a sound wave frequency of 2000 Hz, pulse width of 0.1 s, and source level of 0 dB. The sea surface wind speed is 5 m/s, and the substrate is clay. Based on the Chapman model and the GABIM model, the backscattering RL received by the receiving hydrophone over time is calculated, as shown in Fig. 7(a). The multipath reverberation grazing angle varies over time as shown in Fig. 7(b). The echo grazing angle of a target at a depth of 100 m at any horizontal position varies over time as shown in Fig. 7(b). The serial numbers of the reverberation multipaths in Fig. 7(b) correspond one-to-one with the reverberation paths in Fig. 6(c).

In Fig. 7(a), the RL of seabed backscattering reverberation received simultaneously is significantly lower than that of sea surface backscattering reverberation. The discrepancy primarily arises from the monostatic sonar's proximity to the seabed and distance from the sea surface. The grazing angle of seabed backscattering reverberation decreases significantly faster over time compared to sea surface reverberation (as shown in Fig. 7(b)). Given that the backscattering strength of both sea surface and seabed reverberation decreases with reduced grazing angles, this angular dependence results in the RL of the seafloor backscatter reverberation is smaller than that of the sea surface reverberation.

As demonstrated in Fig. 7(a) and (b), the direct sea surface backscattering reverberation exhibits higher intensity, prolonged duration, and a time-delay-elevation angle structure closely resembling that of near-surface targets. Consequently, such reverberation constitutes the dominant interference for active detection and parameter estimation of near-surface targets by deep-sea deployed sonar systems, owing to its spatial-temporal similarity to target echoes.

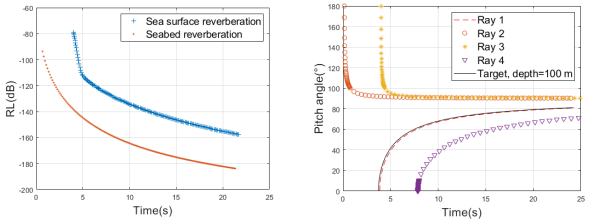

(a) (b)

Figure 7. Multi-path reverberation structure varies with arrival delay. (a) The reverberation intensity varies with time delay; (b) The reverberation pitch angle varies with time delay (The pitch angle is the angle between the direction of the incident wave and the vertical upward normal).

2.4 Deep-sea backscatter reverberation array data simulation model

The previous text completed the forecast of the deep-sea reverberation intensity and the spatiotemporal structure of the arrival based on marine meteorological data and geographic data, and concluded that sea surface backscattering reverberation is the primary interference affecting target detection. This section proposes a method for constructing reverberation array data by combining marine meteorological data, oceanographic data, and sonar parameters.

Assuming that the number of elements in the receiving array is M, and the coordinate of the m-th element relative to the reference element is $\mathbf{p}_m = [p_x, p_y, p_z]^{\mathrm{T}}$. Traditional reverberation modeling theories include point scattering models and cell scattering models [9]. The point scattering model has a clear physical meaning. In this paper, the reverberation data received by the array is constructed based on the point scattering model. Underwater reverberation is the superposition of echoes generated by the scattering of emitted signals from scatterers at the sea surface or seabed interface and within the wa-

ter body, where the point scattering model abstracts the scatterers contributing to the reverberation into individual scattering points. Assuming that the waveform of the transmitted signal is $s(t)$ and its power is one. The number of scatterers contributing to the reverberation is *I*. The waveform of the reverberation signal received by each element at time t can be represented as follows

$$\mathbf{n}(t) = \sum_{i=1}^{I} \begin{bmatrix} A_i s[t - t_i - \tau_1(\Omega_i)] \\ A_i s[t - t_i - \tau_2(\Omega_i)] \\ \vdots \\ A_i s[t - t_i - \tau_M(\Omega_i)] \end{bmatrix}, \tag{8}$$

where A_i is denoted as the amplitude and phase change of the reverberation scattered by the i-th scatterer to the receiving array. t_i is the two-way echo delay of the i-th scatterer scattering reverberation to the position of the reference element. $\Omega_i = (\theta_i, \varphi_i)$ is the spatial angle at which the reverberation scattered by the i-th scatterer reaches the array, θ_i is pitch angle, φ_i is horizontal azimuth. The parameters t_i and Ω_i can be calculated using ray theory. $\tau_m(\Omega_i)$ denotes the time delay difference of the reverberation scattered by the i-th scatterer arriving at the m-th array element relative to the reference element. $\tau_m(\Omega_i)$ can be calculated as

$$\begin{aligned} v_i(\Omega_i) &= -[\sin(\theta_i)\cos(\varphi_i), \sin(\theta_i)\sin(\varphi_i), \cos(\theta_i)]^{\mathrm{T}} \\ \tau_m(\Omega_i) &= [v_i(\Omega_i)]^{\mathrm{T}} \mathbf{p}_m / c \end{aligned}, \tag{9}$$

where c is underwater sound speed. A_i is a complex number and can be expressed as

$$A_i = \sigma_i e^{\mathrm{j}\varphi_i}, \tag{10}$$

where σ_i and φ_i are the amplitude and phase changes caused by the signal being scattered by i-th scattering points. As mentioned earlier, the backscatter reverberation of the sea surface is the main interference, while the scattering of the reverberation on the sea surface is essentially diffuse scattering [10]. According to the central limit theorem, the envelope of the reverberation σ_i satisfies the Rayleigh distribution, and φ_i satisfies a uniform distribution of $0 - 2\pi$. The power of the backscatter reverberation received by the array at time t can be calculated by Eqn. (2) and Eqn. (6), and the power is σ^2_{RL}. Let the number of scattering points that contribute to the reverberation at time t be L, then the σ_l corresponding to these L scattering points generally satisfies the following equation

$$\sigma^2_{\mathrm{RL}} = L\mathrm{E}\left(|\sigma_l|^2\right) \; l = 1, 2 \cdots L. \tag{11}$$

A_i can be calculated by Eqn. (10) and Eqn. (11).

(t_i, Ω_i) reflects the spatiotemporal distribution of the reverberation scattered by the i-th scattering point. The coordinate of the array is $\mathbf{p}_o = [0, 0, Z_N]^{\mathrm{T}}$, Z_N is the depth of the array. The coordinate of the i-th scattering point on the sea surface is $\mathbf{p}_i = [p_{ix}, p_{iy}, 0]^{\mathrm{T}}$. If the scattering points are evenly distributed in the detection area, the maximum value of the horizontal distance of the detection area is $R_{\max}$. Then p_{ix} and p_{iy} are random variables with uniform distribution of minimum and maximum values $-R_{\max}$ and $R_{\max}$, respectively. The arrival time delay t_i and arrival angle Ω_i between points $\mathbf{p}_o$ and $\mathbf{p}_i$ can be calculated using the measured sound speed profile in conjunction with ray model. The flowchart for adding the reverberation waveform scattered by the i-th scattering point to $\mathbf{n}(t)$ is shown in Fig. 8.

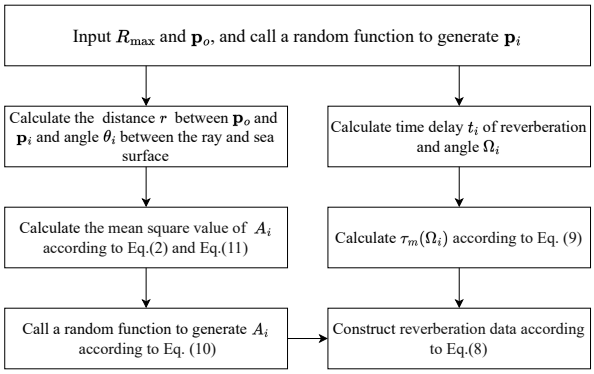

Figure 8. Flowchart for constructing reverberation data.

3. SIMULATION ANALYSIS

In deep sea, if underwater active detection is performed as shown in Fig. 1, the sea surface backscattering reverberation is the main interference. In this section, the sea surface backscattering reverberation generated by different waveforms will be simulated. Assuming that there is a ten-element vertical uniform linear array as the receiving array, and the distance between two adjacent elements equals half the wavelength of the transmitted signal's center frequency. The reference depth of the array is 3000 m.

The simulation environment is assumed to be an isospeed acoustic medium with a sound speed of 1500 m/s, and the sea surface wind speed is 4 m/s. The sea surface backscattering reverberation echoes are simulated within a horizontal range of 10 km. In subsequent analyses, various transmit waveforms will be employed to construct the reverberation data.

The transmitted waveform is chosen as a Linear Frequency Modulated (LFM) signal, whose analytical expression is

$$s(t) = \sin(2\pi f_0 t + \pi \frac{B}{T} t^2), t \in [0, T], \qquad (12)$$

where $f_0 = 1.5\text{kHz},, B = 1\text{kHz}, T = 0.4\text{s}$. Fig. 9 shows the spectrum of the LFM signal and the time waveform, time-frequency representation, and amplitude statistical distribution of reverberation.

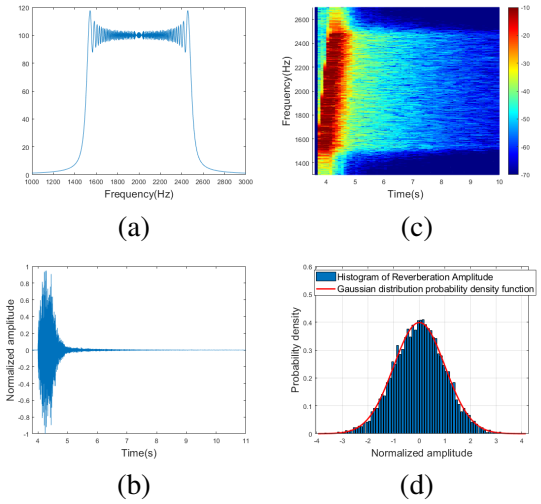

(a) (c) (b) (d)

Figure 9. The spectrum and sea surface back scattering reverberation of LFM transmitted signal. (a)The spectrum of LFM;(b)Time domain of reverberation; (c)Time-frequency domain of reverberation; (d)Reverberation amplitude statistical distribution.

The transmitted waveform is chosen as a Pulse Time-Frequency Modulated (PTFM) signal, whose analytical expression is

$$s(t) = \sin\left[2\pi f_0 (t - \lfloor t/T_p \rfloor T_p) + \pi \frac{B}{T_p} (t - \lfloor t/T_p \rfloor T_p)^2\right], \quad t \in [0, T] \qquad (13)$$

where $f_0 = 1.5\text{kHz}, B = 1\text{kHz}, T = 0.4\text{s}, T_p = 0.04\text{s}$. Fig. 10 shows the spectrum of the PTFM signal and the time waveform, time-frequency representation, and amplitude statistical distribution of reverberation.

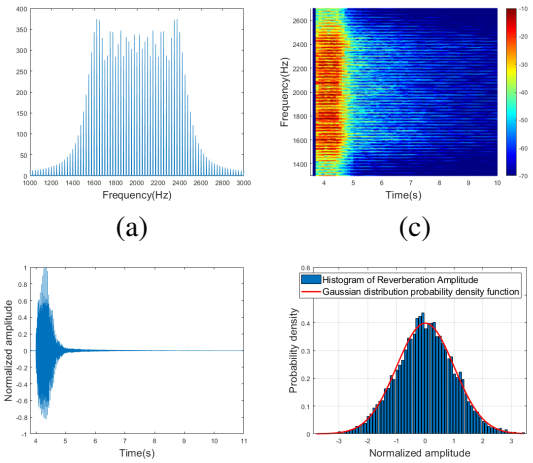

(a) (c) (b) (d)

Figure 10. The spectrum and sea surface back scattering reverberation of PTFM transmitted signal. (a)The spectrum of PTFM;(b)Time domain of reverberation; (c)Time-frequency domain of reverberation; (d)Reverberation amplitude statistical distribution.

Through analysis of Fig. 9(b) and Fig. 10(b), the amplitude of sea surface backscattering reverberation exhibits temporal decay, with decay rates independent of specific waveforms. Comparative analysis between Fig. 9(a) vs. Fig. 9(c), and Fig. 10(a) vs. Fig. 10(c) reveals that the frequency components of reverberation are fundamentally consistent with those of the transmitted signal, and the arrival sequence of reverberation frequency components matches the emission sequence of the transmitted signal's frequency components.

As demonstrated in Fig. 9(d) and Fig. 10(d), the amplitude distribution of sea surface backscattering reverberation generated by different waveforms adheres to a Gaussian distribution. Since sea surface scattering is generally diffuse scattering, where no prominent scatterers exist, amplitude of reverberation follows a Gaussian distribution according to the central limit theorem. Excellent agreement is observed between theoretical predictions and simulation results.

Conventional beamforming method is employed to

draw the Beamforming Time Recording(BTR) of the sea surface backscattering reverberation generated by diverse transmitted waveforms (Fig. 11). Comparative analysis with Fig. 7(b) and Fig. 11 indicates that sea surface backscattering reverberation exhibits notable spatiotemporal distribution structures, reflecting the spatial-temporal characteristics of sea surface scatterers. Clearly, the intensity distribution in BTR displays minimal dependence on the transmitted waveform.

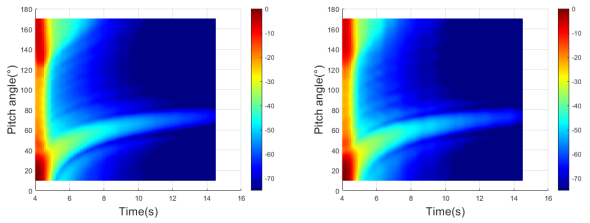

(a) (b)

Figure 11. BTR of diverse transmitted waveforms. (a)LFM; (b)PTFM.

4. CONCLUSION

In this work, A reverberation model for deep-sea surface backscattering reverberation is developed by integrating ray theory, Chapman theory and GABIM theory. The analysis of spatiotemporal distribution structures of reverberation reveals that sea surface backscattering reverberation constitute the dominant interference source in active detection of near-surface targets, because of the high intensity, prolonged temporal decay and similar characteristics of spatiotemporal distribution with targets. At the same time, A point scattering model-based method is proposed to synthesize array-received sea surface backscattering reverberation data. This method takes into account the relationships between reverberation data and sonar parameters (waveform, source level, etc.), oceanographic-meteorological parameters (wave height, wind speed, etc.), and marine geological parameters (water depth, substrate types, sound speed profile, etc.). By acquiring such environmental information for target sea areas through oceanographic satellites or other platforms, and subsequently applying it to the reverberation modeling approach, the generated data can be utilized to construct comprehensive datasets and optimize the intelligent algorithm models for sonar systems. This provides crucial data for the design of near-seabed sonar systems.

5. ACKNOWLEDGMENTS

This work is supported by the National Key R&D Program of China under Grant 2022YFC3101900.

6. REFERENCES

[1] R. K. McCargar and L. M. Zurk, "Depth-based suppression of moving interference with vertical line arrays in the deep ocean," *The Journal of the Acoustical Society of America*, vol. 132, no. 3_Supplement, pp. 2081–2081, 2012.

[2] R. Wei, X. Ma, and X. Li, "Depth estimation of deep water moving source based on ray separation," *Applied Acoustics*, vol. 174, p. 107739, 2021.

[3] C. Chen, H. Ruang, C. Chi, Y. Li, and S. Jin, "Estimating target depth for deep-sea active sonars through channel-impulse-response matching," in *OCEANS 2024-Singapore*, pp. 1–5, IEEE, 2024.

[4] L. Bjørnø, T. Neighbors, and D. Bradley, *Applied underwater acoustics*. Elsevier, 2017.

[5] D. R. Jackson, R. I. Odom, M. L. Boyd, and A. N. Ivakin, "A geoacoustic bottom interaction model (gabim)," *IEEE Journal of Oceanic Engineering*, vol. 35, no. 3, pp. 603–617, 2010.

[6] X. Runze, D. Rui, Y. Kunde, M. Yuanliang, and G. Yue, "Modeling and analysis of monostatic incoherent boundary reverberation intensity in deep water," *ACTA ACUSTICA*, vol. 46, no. 6, pp. 926–938, 2022.

[7] D. Jackson and M. Richardson, *High-frequency seafloor acoustics*. Springer Science & Business Media, 2007.

[8] F. B. Jensen, W. A. Kuperman, M. B. Porter, H. Schmidt, and A. Tolstoy, *Computational ocean acoustics*, vol. 2011. Springer, 2011.

[9] Q.-y. Sun, H.-y. Wang, X.-h. Shen, W.-z. Ning, and X.-y. Fu, "Research on the statistical modeling and simulation for interface reverberation," in *2010 3rd International Conference on Computer Science and Information Technology*, vol. 9, pp. 566–570, IEEE, 2010.

[10] P. Gerstoft and H. Schmidt, "A boundary element approach to ocean seismoacoustic facet reverberation," *The Journal of the Acoustical Society of America*, vol. 89, no. 4, pp. 1629–1642, 1991.